Sigma Bond Activation by Cooperative Interaction with ns^2 Atoms: $Al^+ + nH_2$

Stephanie B. Sharp, Blake Lemoine, and Gregory I. Gellene*

Department of Chemistry and Biochemistry Texas Tech University Lubbock, Texas 79409-1061

Received: May 14, 1999; In Final Form: August 16, 1999

The reactions of $Al^+ + nH_2$ to produce $AlH_2^+(H_2)_{n-1}$ have been studied by high-level ab initio electronic structure techniques motivated by the σ bond activation by cooperative interaction observed experimentally and theoretically for the isovalent $B^+ + nH_2$ reaction systems. For $n = 1$, the reaction proceeds stepwise: first breaking the H_2 bond and forming one AlH bond followed by the formation of the second AlH bond. This process has an activation energy of 85.0 kcal/mol. For $n = 2$, the reaction proceeds via a pericyclic mechanism through a planar, cyclic transition state where two H_2 bonds are broken simultaneously while two AlH bonds and one new H_2 bond are formed. The activation energy for this process decreases from the $n = 1$ value to about 55.0 kcal/mol. These two cases are qualitatively very similar to what was observed for $B^+ + nH_2$ with the major quantitative differences being that corresponding activation energies were 30−40 kcal/mol lower and reaction energetics were 60−80 kcal/mol more exothermic in the boron systems. For $n = 3$, no additional activation energy lowering was observed with Al^+, which contrasts significantly with the behavior observed with B^+. This difference is rationalized in terms of the special ability of boron to form strong three center−two electron bonds.

Introduction

Recently, experimental[1] and theoretical[2] investigations have revealed remarkable and unexpected chemistry for the reaction of $B^+(2s^2, {}^1S_g)$ and H_2. Formation of the covalently bound, linear, centrosymmetric molecule, BH_2^+, is exothermic by about 56 kcal/mol with respect to B^+ and H_2. However, the presence of a 57 kcal/mol reaction barrier effectively prevents the reaction from proceeding efficiently, and only weakly bound, electrostatic complexes, $B^+(H_2)$, formed by three-body association reactions, are observed. With increased hydrogen pressure and/or decreased temperature, additional H_2 molecules can be electrostatically complexed to B^+. Computational results indicate that the incremental binding energy decreases with each addition, covering the range of 3.4−0.8 kcal/mol for $n = 1-4$ when zero point energy effects are included. These results are in good agreement with the experimentally determined binding energies for the first and second H_2 addition; the two electrostatic complexes for which experimental binding energies are available. The electrostatic binding energy of the third H_2 molecule was not determined experimentally because the $B^+(H_2)_3$ complex reacted with near zero activation energy to produce the BH_2^+ ion. Interestingly, interaction of this ion with up to two additional H_2 molecules was predicted to result in strong bonding (14−18 kcal/mol),[2−4] attributable to the formation of three center-two electron (3c−2e) bonds and this was observed experimentally[1].

The most interesting question, however, was how the weak, electrostatic bonding of three H_2 molecules to B^+ could allow a 57 kcal/mol activation energy barrier to be surmounted. It seemed likely that energetic considerations alone could not account for this effect and that a mechanistic change was involved. The computational identification of the transition state for reactions involving one to three hydrogen molecules[2] showed that, indeed, the mechanism and associated activation energy depended dramatically on the number of hydrogen molecules involved. With one hydrogen, the reaction proceeds stepwise: first breaking the H_2 bond and forming one BH bond, followed by the formation of the second BH bond. With the addition of a second hydrogen molecule, the reaction proceeds via a pericyclic mechanism through a planar cyclic transition state where two H_2 bonds are broken while simultaneously two BH bonds and one new H_2 bond are formed. This mechanistic change lowered the activation energy by nearly 80%. The addition of a third H_2 removed more than 70% of the remaining activation energy with a transition state that is geometrically very similar to that of the electrostatic complex. Although this case proceeds through a true insertion mechanism, the insertion occurs late in the reaction after over 75% of the exothermicity has been realized.

A detailed study of the evolution of the occupied molecular orbitals along the various reaction paths provided a full understanding of the mechanisms and ensuing activation energy changes. For all electrostatic complexes, the highest occupied molecular orbital (HOMO) is one that has a node between the B^+ ion and the H_2 molecule(s). To activate the H_2 molecule, this node has to be "maneuvered" to intersect an H_2 bond. With a single hydrogen molecule present, this can be accomplished by allowing the B^+ ion to interact strongly with only one hydrogen of the H_2 molecule, causing the energy requirement of breaking the H_2 bond to be offset by the formation of only one BH bond. With the addition of a second hydrogen molecule, the node of the HOMO is positioned at the transition state to intersect both H_2 bonds, allowing the B^+ ion to interact strongly with two hydrogen atoms. With three hydrogen molecules present, the node in the HOMO begins to intersect all three H_2 bonds at the transition state and the B^+ ion interacts equivalently with three hydrogen atoms.

Once the mechanism for this unusual σ bond activation was well understood, an interesting question naturally arose: is B^+ essential or will the mechanism operate with other ns^2 electron configuration atoms? The present work takes a first step toward answering this question by examining the interaction of Al^+

10.1021/jp991587a CCC: $18.00
Published on Web 09/29/1999

with nH$_2$ (n = 1−4). Because Al$^+$ is isovalent with B$^+$, the topologies of relevant molecular orbitals for the aluminum systems are expected to be similar to the corresponding boron systems, although the energetics could be quite different. For example, in the boron work it was not clear how much of the activation energy lowering could be attributed to the strong 3c−2e bonds that would be formed after insertion when two or three hydrogen molecules were present. Although 3c−2e bonding has been observed for aluminum,[5] this bonding motif is certainly less prominent for aluminum than it is for boron.

A preliminary account of some of these calculations was published previously [6] in conjunction with an experimental gas phase ion chemistry study that searched unsuccessfully for Al$^+$ insertion chemistry analogous to that observed for B$^+$. In that work only reactants and products were characterized and no information on the intervening transition states was provided. Further, electron correlation was considered only at the MP2 level, which had proved to be not entirely satisfactory in describing the BH$_2^+$(H$_2$)$_n$ ions. Beyond that study, AlH$_2^+$ appears to have been considered previously in only one low-level ab initio study,[7] and we are unaware of any experimental spectroscopic information. The present work extends our previous study by fully characterizing transition states, electrostatic complexes, and inserted molecules using couple cluster and multireference techniques in addition to MP2. This information allows a meaningful comparison between the chemistry of Al$^+$/nH$_2$ and B$^+$/nH$_2$ to be made.

Methods

Preliminary geometry optimizations and stationary point characterizations were performed using the aug-cc-pVDZ basis set[8] with final geometry optimizations and characterizations being performed with the aug-cc-pVTZ basis set.[9] The former basis set is of double-ζ quality, the latter is of triple-ζ quality, and both are augmented by diffuse functions that are required to describe polarizability properly, which is particularly important for the electrostatic complexes. No significant qualitative differences between the results obtained with the two basis sets were observed. For aluminum, the triple-ζ basis set consists of a (15s9p2d1f) set of primitive Gaussian functions contracted to [5s4p2d1f] and augmented by an uncontracted (1s1p1d1f) set of functions. For hydrogen, the triple-ζ basis set consists of a (7s2p1d) set of primitive Gaussian functions contracted to [3s2p1d] and augmented by an uncontracted (1s1p1d) set of diffuse functions. Pure spherical harmonic basis functions were used throughout.

Stationary points on the electrostatic complex, Al$^+$(H$_2$)$_n$, and inserted molecule, AlH$_2^+$(H$_2$)$_{n-1}$, hypersurfaces were located and characterized by MP2 perturbation theory applied to a Hartree−Fock (HF) wave function with frozen core electrons. Analytical first derivatives were used to optimize geometric structures to a residual root-mean-square force of less than 10^{-6} hartree/bohr, and analytical second derivatives were used to characterize a stationary point as a local minimum or a transition state. For each transition state identified, the local reaction coordinate was determined by displacing the geometry slightly in the direction of the eigenvector associated with the imaginary frequency (both positive and negative) and following the gradient to a subsequent stationary point.

This general computational approach was followed in all cases except for characterizing the transition state region of the n = 1, Al$^+$/H$_2$ system. This region of that potential energy surface is necessarily multiconfigurational and cannot be described well by MP2 calculations based on a single configuration wave function. Instead, complete active space (CAS) multiconfigurational self-consistent-field (MCSCF)[10,11] calculations followed by internally contracted configuration interaction in the single and double space (MRCISD)[12,13] were performed. In the MCSCF calculations, the $1s^2 2s^2 2p^6$ core electron configuration of Al was held frozen and the four valence electrons were distributed among the six orbitals arising from the 3s and 3p atomic orbitals of Al and the 1s orbitals of each hydrogen atom.

At each stationary point identified by the MP2 calculations, MRCISD and coupled cluster with single and double substitutions and a perturbative treatment of triple substitutions (CCSD(T))[14] calculations were performed. Because MRCISD is not size extensive, energies can be compared properly only when the same number of H$_2$ molecules are considered (i.e., the supermolecule approach), which was taken to be 3 in this study. Davidson[15] has proposed a correction (Q) to partially compensate for the size nonextensivity of MRCISD calculations and MRCISD+Q energies will be reported also as appropriate. The MP2 and CCSD(T) calculations were performed with the GAUSSIAN 94 suite of programs[16] and the MRCISD calculations were performed with the MOLPRO[17] electronic structure package. All calculations were performed on a DEC alpha workstation.

Results

To simplify comparisons between the properties of various Al$^+$/nH$_2$ stationary points and the corresponding B$^+$/nH$_2$ stationary points, only a subset of internal coordinates and harmonic frequencies will be reported here. A full description of the optimized geometries and harmonic frequencies will be provided as Supporting Information. The coordinates R, r(H$_2$), and $\theta_{R,r(H_2)}$ will be used to denote the distance between Al$^+$ and the midpoint of an H$_2$ molecule, the H$_2$ bond length, and the angle between R and r(H$_2$), respectively. The coordinates r(AlH) and θ_{HAlH} will denote the AlH bond length and HAlH bond angle in the AlH$_2^+$ moiety of a AlH$_2^+$(H$_2$)$_{n-1}$ molecule or the transition state forming it. The angle formed by two different R coordinates will be denoted $\theta_{R,R'}$. The electronic energy of Al$^+$(H$_2$)$_n$ and AlH$_2^+$(H$_2$)$_{n-1}$ and harmonic zero point energies (ZPEs) are reported relative to the energies of the infinitely separated Al$^+$ + nH$_2$ reactants. Unscaled MP2 harmonic frequencies are used in the calculation of ZPEs. Variations in the H$_2$ bond length and harmonic stretching frequency are important indicators of 3c−2e bonding, and the present results are compared with the previously reported[2] MP2/aug-cc-pVTZ values of 0.7374 Å and 4518 cm^{-1}, respectively for isolated H$_2$.

Al$^+$(H$_2$) and AlH$_2^+$. Geometric and energetic parameters characterizing stationary points on this hypersurface are summarized in Table 1 and illustrated in Figure 1. The electrostatic complex is calculated to be T-shaped (C_{2v}) with the H$_2$ moiety little changed from its isolated characteristics (Δr(H$_2$) = 0.0044 Å, $\Delta\omega$(H$_2$) = −70 cm^{-1}) and R equal to about 3.01 Å. Calculated electronic binding energies fall into two groups: a low value near −1.65 kcal/mol with MP2 and MRCISD+Q techniques and a value about 85% larger with CCSD(T) and MRCISD techniques. Inclusion of MP2 harmonic ZPE predicts an adiabatic dissociation energy (D_0) that is decreased from D_e by 0.69 kcal/mol. The covalently bound, inserted AlH$_2^+$ molecule is calculated to be a linear symmetric ($D_{\infty h}$) molecule with r(AlH) equal to 1.55 Å. Calculated D_e values by the four methods investigated agree to within 1 kcal/mol, predicting a value of about +10 kcal/mol. The positive sign of this value

TABLE 1: Calculated Geometry[a] and Relative Energy for $Al^+(H_2)$ and AlH_2^+ Stationary Points

property	electrostatic complex	transition state[b]	inserted molecule
point group	C_{2v}	C_s	$D_{\infty h}$
R (Å)	3.0113		
$r(H_2)$ (Å)	0.7418	2.8072	
r(AlH) (Å)		1.6197	1.551
relative energy[c]			
MP2	−1.75		+9.60
CCSD(T)	−3.10		+9.45
MRCISD	−2.81	+88.76	+10.22
MRCISD+Q	−1.53	+88.39	+10.83
relative ZPE[c]			
per-H_2	+0.69[d]	−4.61[e]	+1.29[d]
per-D_2	+0.49[d]	−3.24[e]	+1.03[d]

[a]Optimized at the MP2/aug-cc-pVTZ level of theory. [b]Angle between $r(H_2)$ and r(AlH) is 93.3°. [c]Relative to $Al^+ + H_2$ in kcal/mol. [d]At the MP2/aug-cc-pVTZ level of theory. [e]At the MRCISD/aug-cc-pVTZ level of theory.

means that AlH_2^+ is less stable than the $Al^+ + H_2$ reactants. Despite this thermodynamic instability, AlH_2^+ lies in a relatively deep local potential energy minimum characterized by MP2 harmonic frequencies of 2085, 582, and 2174 cm^{-1} for the symmetric stretching, bending, and asymmetric stretching modes, respectively. Harmonic ZPE considerations decrease the stability of AlH_2^+ by about 1.3 kcal/mol. The depth of the AlH_2^+ potential well is established by the energy of the transition state for AlH_2^+ formation. This transition state lies about 88.8 kcal/mol above the $Al^+ + H_2$ reactants or about 78.5 kcal/mol above the AlH_2^+ product based on MRCISD calculations. The inclusion of ZPE considerations decreases the energy of this transition state by about 3.8 kcal/mol with respect to $Al^+ + H_2$. The geometry of this transition state has a low symmetry, C_s structure with very inequivalent hydrogen atoms. One r(AlH) has a bonding distance of 1.62 Å, and the other r(AlH) has a very long distance of 3.32 Å.

$Al^+(H_2)_2$ and $AlH_2^+(H_2)$. Geometric and energy parameters characterizing this hypersurface are summarized in Table 2 and illustrated in Figure 2. The electrostatic complex is calculated at the MP2 level to have a C_s geometry with each H_2 adopting a T- or near T-shape structure with the Al^+ ion. These two H_2 molecules lie on the same "side" of the Al^+ ion with R equal to approximately 3.0 Å and $\theta_{R,R'}$ equal to about 66°. The bond length and vibrational frequencies of the H_2 molecules in the complex are changed by only +0.0045 Å and −71 cm^{-1} from the isolated H_2 values. The calculated D_e values again fall into two groups with the CCSD(T) and MRCISD values being about 70% larger than the MP2 and MRCISD+Q values. Inclusion of a harmonic ZPE consideration predicts an adiabatic D_0 that is 1.74 kcal/mol less than D_e. The transition state for forming the covalently bound AlH_2^+ ion has C_{2v} symmetry with the equivalent H_2 bond lengths increased by almost 0.5 Å to about 1.2 Å and r(AlH) decreased to almost the equilibrium AlH_2^+ values. The covalent molecular ion is formed from this transition state through a pericyclic mechanism where simultaneously two AlH bonds are formed, two H_2 bonds are formed, and a new H_2 bond is formed. This mechanism implies that the two hydrogen atoms that ultimately participate in the two AlH bonds of $AlH_2^+(H_2)$ originate from different hydrogen molecules, as do the two hydrogen atoms that ultimately form the H_2. In the covalently bound molecular ion, the interaction of AlH_2^+ with H_2 induces only small distortions in each subunit with $r(H_2)$ increasing by about 0.02 Å and θ_{HAlH} decreasing by about 16°.

$Al^+(H_2)_3$ and $AlH_2^+(H_2)_2$. Geometric and energy parameters characterizing this hypersurface are summarized in Table 3 and illustrated in Figure 3. The electrostatic complex is calculated at the MP2 level to have C_3 symmetry with the R and $r(H_2)$ values being comparable to those of $Al^+(H_2)$ and $Al^+(H_2)_2$. As was the case with the other electrostatic complexes, each H_2 adopts a near T-shape geometry with the Al^+ ion with $\theta_{R,R'}$ equal to 65.6°. Again, the calculated D_e values tend to fall in two groups, with MP2 and MRCISD+Q predicting lower values and CCSD(T) and MRCISD predicting higher values. The agreement between the CCSD(T) and MRCISD values is less than it was for $Al^+(H_2)$ and $Al^+(H_2)_2$. Inclusion of harmonic ZPE considerations predicts an adiabatic D_0 that is 3.06 kcal/mol less than D_e. The transition state for forming the covalently bound AlH_2^+ ion has C_s symmetry and, in essence, is very similar to the two H_2 case. Here, two H_2 molecules participate in the pericyclic transition state and the third H_2 lies considerably further from the Al^+ ion and has an $r(H_2)$ only about 0.022 Å larger than the equilibrium H_2 value. From this transition state, the covalent AlH_2^+ is formed as it was in the two H_2 case, with R for the third H_2 decreasing only slightly in the process. The interaction of AlH_2^+ with a second H_2 induces slightly larger distortions in each subunit, with $r(H_2)$ increasing by an additional about 0.013 Å and θ_{HAlH} decreasing by an additional 6.3° from the $AlH_2^+(H_2)$ values.

Discussion

Instructive trends in the results can be identified by grouping the systems as electrostatic complexes, covalent molecular ions, and the intervening transition states. It is also instructive to consider the relative energetics for the stepwise addition of each H_2 molecule within these groups. Although this information is available implicitly in Tables 1−3, it is provided in Table 4 for convenience. Constructing Table 4 required choosing the D_e values of a particular method. Energies from CCSD(T) calculations generally are considered more reliable than those from MP2 because CCSD(T) captures significantly more electron correlation. Although CCSD(T) and MRCISD capture comparable amounts of electron correlation, as judged by the absolute total energies, the approximate 0.65 kcal/mol per subunit discrepancy between MRCISD and MRCISD+Q relative energies for the electrostatic complexes (where Al^+ and H_2 are the subunits) and the covalent molecular ions (where AlH_2^+ and H_2 are the subunits) is about 3 times larger than that observed for the isovalent B^+/nH_2 systems. Noting that, with frozen core electrons, the electronic structure of B^+/nH_2 and Al^+/nH_2 are very similar, it seems that correcting for the nonsize extensivity of MRCISD is more difficult in the Al^+/nH_2 system. Thus, CCSD(T) values for relative energy were used in the construction of Table 4 with the exception of the Al^+/H_2 transition state, for which MRCISD calculations are required. In the following discussion, comparisons to experiment and the previously calculated results for the isovalent B^+/nH_2 systems will be made as appropriate.

Electrostatic Complexes. In all cases, the H_2 species adopts a T- or a near T-shape geometry with respect to Al^+, which is the attractive orientation of the H_2 quadrupole. The positions of the H_2 molecules are also constant among the complexes with R being about 3.0 Å, $\theta_{R,R'}$ being 65.5°, and the H_2 molecules adopting the most attractive, near T-shape structures with respect to each other. Compared to those for B^+/nH_2, the R and $\theta_{R,R'}$ values for Al^+/nH_2 are about 0.75 Å longer and 12° smaller, respectively. Taken together, these geometric changes place the centers of H_2 molecules about 3.2 Å apart, which is very close

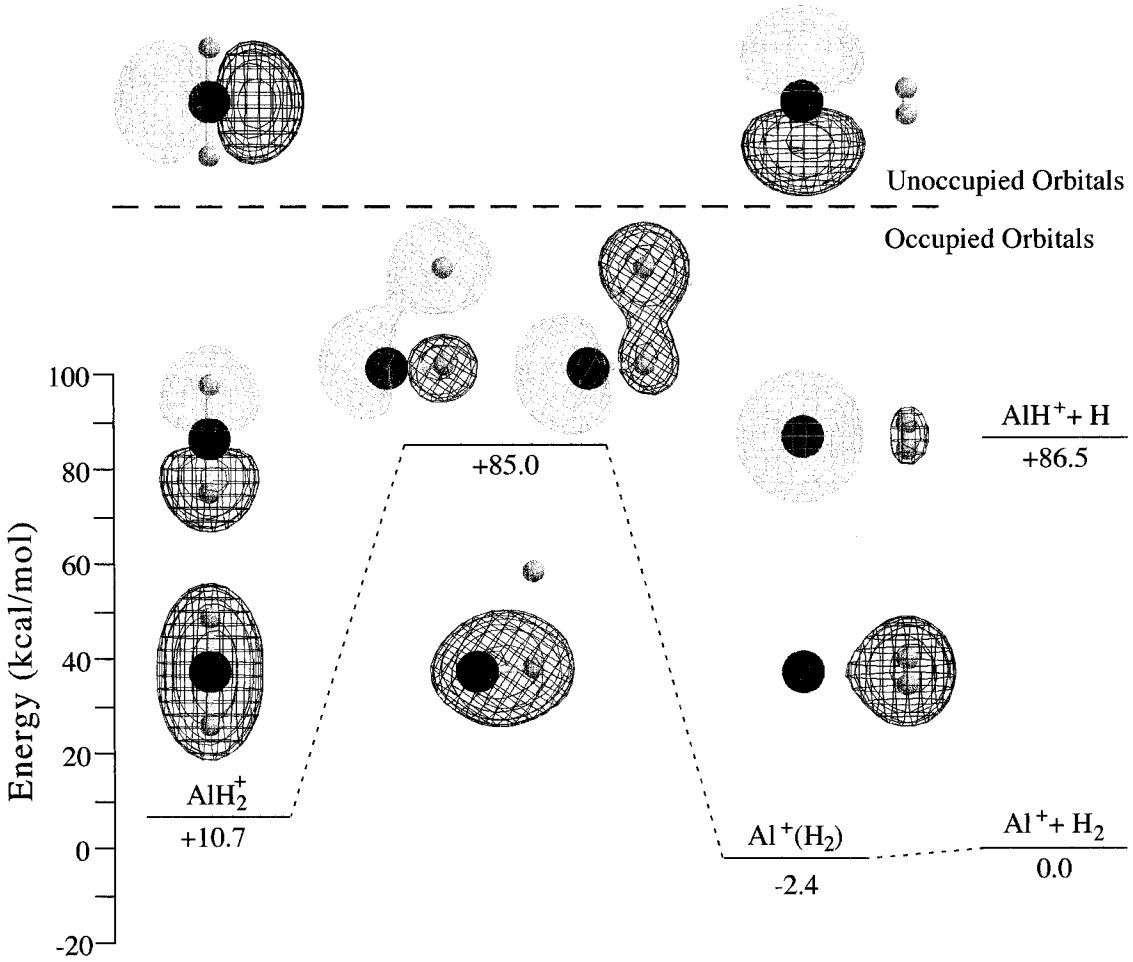

Figure 1. Relative energy of stationary points on the minimum energy path for $Al^+ + H_2 \rightarrow AlH_2^+$ calculated at the CCSD(T)/aug-cc-pVTZ level of theory with harmonic ZPE added for the *per*-H_2 species at the MP2/aug-cc-pVTZ level of theory. The transition state and $AlH^+ + H$ energy were calculated at the MRCISD/aug-cc-pVTZ level of theory. The orbitals pictured for reactants and products are the two highest occupied and lowest unoccupied valence orbitals which illustrate that the energetic barrier arises from the symmetry correlation of the HOMO of the reactants with the LUMO of the products and *vice versa*. The orbitals pictured for the transition state are the lowest occupied and the two nearly equal energy orbitals that comprise the major configurations of the MCSCF wave function. The energy scale does not apply to the orbitals.

TABLE 2: Calculated Geometry[a] and Relative Energy for $Al^+(H_2)_2$ and $AlH_2^+(H_2)$ Stationary Points

property	electrostatic complex[b]	transition state	inserted molecule
point group	C_s	C_{2v}	C_{2v}
R (Å)	2.977 (∥) 3.008 (⊥)	1.753	2.074
$r(H_2)$ (Å)	0.7420 (∥) 0.7419 (⊥)	1.199	0.7576
r(AlH) (Å)		1.658	1.543
θ_{HAlH} (deg)		98.9	164.3
$\theta_{R,r(H_2)}$ (deg)	90.9 (∥) 90.0 (⊥)	71.1	90.0
$\theta_{R,R'}$ (deg)	65.6	58.9	
relative energy[c]			
MP2	−3.61	+53.12	+1.23
CCSD(T)	−6.32	+49.54	−0.21
MRCISD	−5.13	+50.65	+1.47
MRCISD+Q	−3.15	+52.13	+2.71
relative ZPE[c]			
per-H_2	+1.74	+2.95	+4.27
per-D_2	+1.24	+2.24	+3.16

[a] Optimized at MP2/aug-cc-pVTZ level of theory. [b](∥) and (⊥) refer to H_2 molecules parallel and perpendicular to the plane of symmetry, respectively. [c]Relative to $Al^+ + 2H_2$ in kcal/mol.

to the equilibrium $(H_2)_2$ separation.[18] This suggests that H_2/H_2 interactions may contribute to determining the equilibrium structures. This interpretation is supported by the increase in incremental H_2 binding energy for $n = 1-3$. Although it is possible that this binding energy increase results from basis set superposition error (BSSE), calculations on $(H_2)_2$ indicate that the BSSE correction with the aug-cc-pVTZ basis set is only 0.01 kcal/mol[18] and the incremental binding energy for $n = 4$, which would be expected to have the largest BSSE, decreases. This decrease with $n = 4$ was also observed in the B^+/nH_2 system[2] and probably results from each H_2 molecule no longer being able to interact with its own empty *p*-orbital on Al^+. Compared to the available experimental information,[1] the calculated electrostatic binding energies of H_2 to Al^+ and to $Al^+(H_2)$ are about 1 kcal/mol too large.

Covalent Bond Formation. The only other computational study of AlH_2^+ of which we are aware[7] also determined the ion to have a linear centrosymmetric structure. However, no binding energies were reported in that study that could be compared to the present value of +10.7 kcal/mol. The positive binding energy indicates that AlH_2^+ is less stable than $Al^+ + H_2$ and contrasts strongly with the −55.9 kcal/mol binding energy[2] calculated for BH_2^+. This is a substantially larger difference than that between the D_0 of AlH^+ and BH^+, which favors BH^+ by only about 26.2 kcal/mol,[19] indicating that the remaining difference in binding energy (40.4 kcal/mol) arises from the bonding of the second hydrogen atom. Binding of the first and second H_2 to AlH_2^+ is calculated to be exothermic by

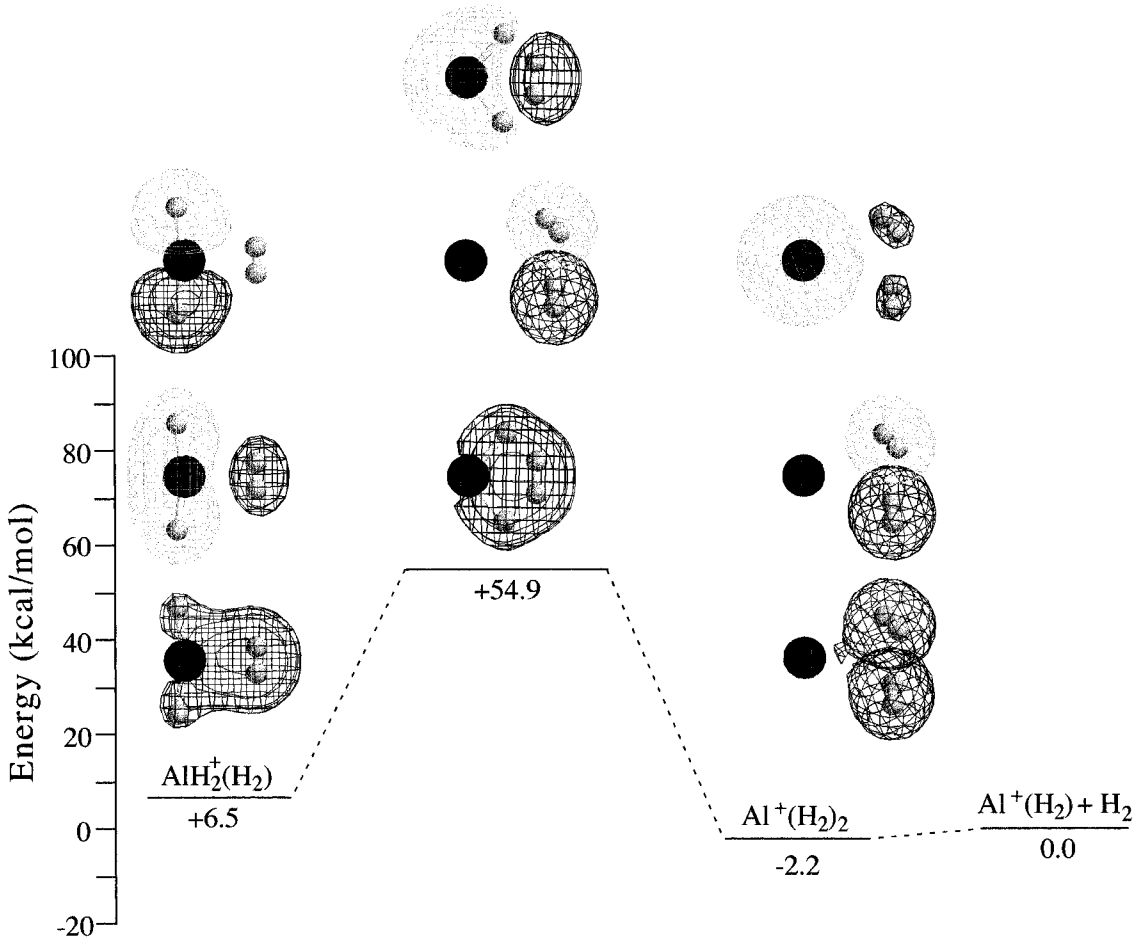

Figure 2. Relative energy of stationary points on the minimum energy path for $Al^+(H_2) + H_2 \rightarrow AlH_2^+(H_2)$ calculated at the CCSD(T)/aug-cc-pVTZ level of theory with harmonic ZPE added for the *per*-H_2 species at the MP2/aug-cc-pVTZ level of theory. The orbitals pictured show the evolution of the highest three occupied valence orbitals along the reaction path. The energy scale does not apply to the orbitals.

TABLE 3: Calculated Geometry[a] and Relative Energy for $Al^+(H_2)_3$ and $AlH_2^+(H_2)_2$ Stationary Points

property	electrostatic complex	transition state[b]	inserted molecule
point group	C_3	C_s	C_{2v}
R (Å)	2.969	2.129 (1) 1.706 (2)	2.093
r(H_2) (Å)	0.7422	0.7591 (1) 1.1813 (2)	0.7707
r(AlH) (Å)		2.129 (1) 1.644 (2)	1.551
θ_{HAlH} (deg)		101.2	158.0
$\theta_{R,r(H_2)}$ (deg)	89.2	85.0 (1) 74.0 (2)	90.0
$\theta_{R,R'}$ (deg)	65.5	61.9 (1) 79.6 (2)	83.1
relative energy[c]			
MP2	−5.60	+46.83	−7.20
CCSD(T)	−9.69	+42.43	−10.19
MRCISD	−7.44	+45.87	−7.39
MRCISD+Q	−5.00	+46.04	−5.70
relative ZPE[c]			
per-H_2	+3.06	+6.19	+7.61
per-D_2	+2.19	+4.50	+5.55

[a] Optimized at the MP2/aug-cc-pVTZ level of theory. [b](1) and (2) refer to the symmetry unique and equivalent H_2 species, respectively. [c]Relative to $Al^+ + 3H_2$ in kcal/mol.

6.7 kcal/mol, which is about 3 times larger than the binding energy of H_2 to Al^+, but less than about one-third of the binding energy of H_2 to BH_2^+ or $BH_2^+(H_2)$. In the case of BH_2^+ or $BH_2^+(H_2)$, the strong binding of H_2 could be attributed to the formation of 3c−2e bonds,[2−4] as indicated by a long $r(H_2)$ value (0.81 or 0.82 Å) and a low H_2 stretching frequency (3579 or 3454 cm^{-1})[2]. A 3c−2e bonding description does not seem appropriate for $AlH_2^+(H_2)_{1,2}$ where $r(H_2)$ is about 0.76 or 0.77 Å, respectively, and the H_2 stretching frequency is about 4231 or 4233 cm^{-1}, respectively. Instead, the increased binding energy of H_2 to AlH_2^+ and $AlH_2^+(H_2)$, as compared to Al^+, probably is best attributed to a decreased effective size of Al in AlH_2^+, induced by the sp-orbital hybridization in the covalent bonds with H, which allows R to decrease by about 0.9 Å. This effect can be seen by comparing the orbital plots in Figure 1.

Transition State Formation. The transition state for AlH_2^+ formation from $Al^+ + H_2$ is calculated to be 85.0 kcal/mol, which is only 1.5 kcal/mol below the energy of $AlH^+ + H$. This energetic result, coupled with the transition state structure having the shorter r(AlH) (1.620 Å) essentially equal to the equilibrium bond length of AlH^+ (1.617 Å), supports the mechanistic interpretation of sequential bond formation for this reaction. This situation is completely analogous to the B^+/H_2 system, with the most significant difference being that the activation barrier for Al^+/H_2 is about 30 kcal/mol greater than that for B^+/H_2.

Following the trend established with the B^+/nH_2 systems, the activation energy for the $Al^+/2H_2$ system decreases about 30 kcal/mol (35% decrease) from the Al^+/H_2 value with a substantial mechanistic change. With two H_2 molecules, the reaction proceeds through a concerted, pericyclic mechanism. Figure 2 shows that in this transition state the node in the HOMO is maneuvered to bisect both H_2 bonds, causing them

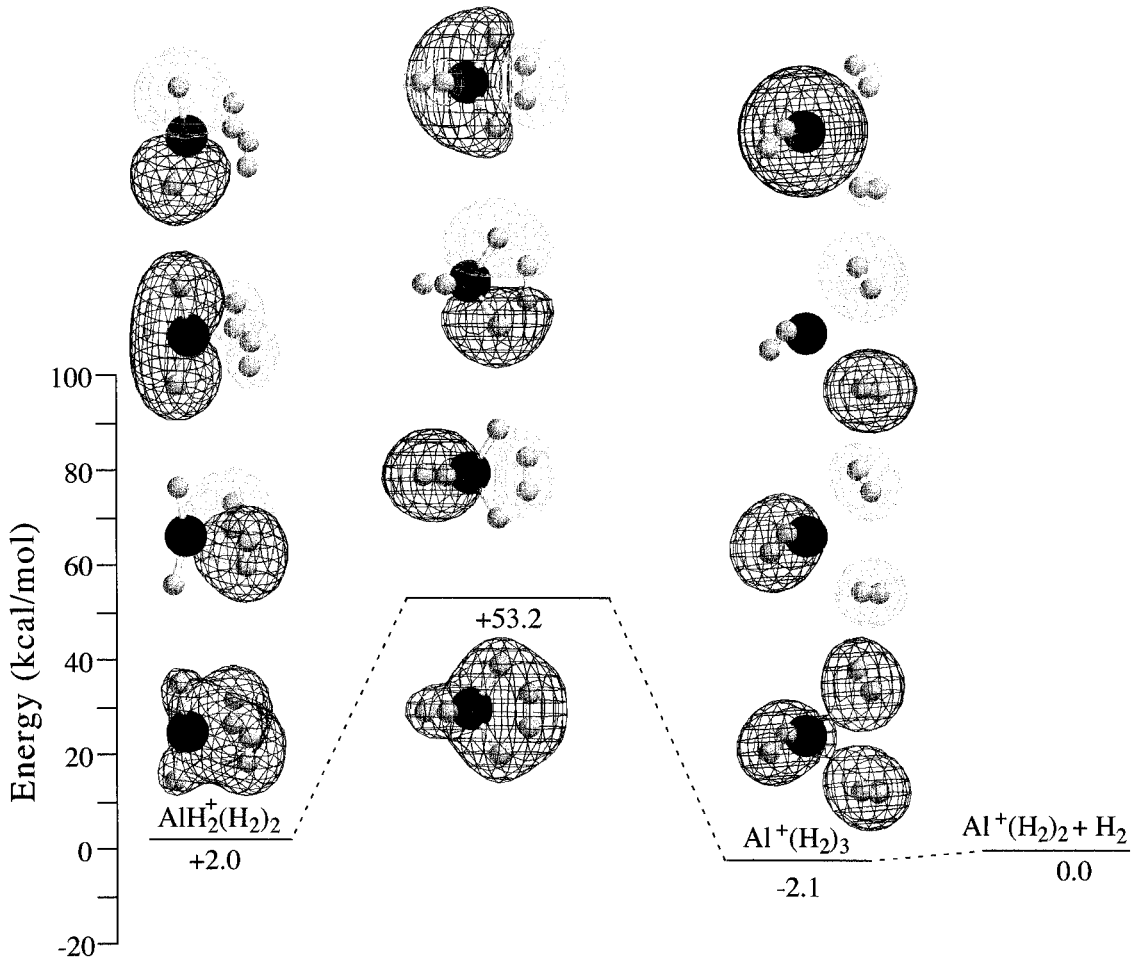

Figure 3. Relative energy of stationary points on the minimum energy path for $Al^+(H_2)_2 + H_2 \rightarrow AlH_2^+(H_2)_2$ calculated at the CCSD(T)/aug-cc-pVTZ level of theory with harmonic ZPE added for the *per*-H_2 species at the MP2/aug-cc-pVTZ level of theory. The orbitals pictured show the evolution of the highest four occupied valence orbitals along the reaction path. The energy scale does not apply to the orbitals.

TABLE 4: Calculated Energy Changes (kcal/mol) for the Indicated Reactions

reaction	electronic[a]	*per*-H_2[b]	*per*-D_2[b]
Electrostatic Complexes			
$Al^+ + H_2 \rightarrow Al^+(H_2)$	−3.10	−2.41 (−1.35 ± 0.15)[c]	−2.61
$Al^+(H_2) + H_2 \rightarrow Al^+(H_2)_2$	−3.22	−2.17 (−1.10 ± 0.15)[c]	−2.47
$Al^+(H_2)_2 + H_2 \rightarrow Al^+(H_2)_3$	−3.37	−2.05	−2.42
$Al^+(H_2)_3 + H_2 \rightarrow Al^+(H_2)_4$	−3.17	−2.02	−2.36
Covalent Molecules			
$Al^+ + H_2 \rightarrow AlH^+ + H$	+88.32[d]	+84.48	+85.64
$Al^+ + H_2 \rightarrow AlH_2^+$	+9.45	+10.74	+10.48
$AlH_2^+ + H_2 \rightarrow AlH_2^+(H_2)$	−9.66	−6.68	−7.53
$AlH_2^+(H_2) + H_2 \rightarrow AlH_2^+(H_2)_2$	−9.98	−6.64	−7.59
Transition States			
$Al^+ + H_2 \rightarrow (Al^+(H_2))^\dagger$	+88.76[e]	+85.01[e]	+85.52
$Al^+(H_2) + H_2 \rightarrow (Al^+(H_2)_2)^\dagger$	+52.64	+54.90	+54.39
$Al^+(H_2)_2 + H_2 \rightarrow (Al^+(H_2)_3)^\dagger$	+48.75	+53.20	+52.01

[a] Electronic energy calculated at the CCSD(T)/aug-cc-pVTZ//MP2/aug-cc-pVTZ level of theory except where otherwise noted. [b] Zero point energy calculated at the MP2/aug-cc-pVTZ level of theory assuming harmonic frequencies. [c] Experimental values from ref 6. [d] MRCISD/aug-cc-pVTZ value is 90.3 kcal/mol. [e] At the MRCISD/aug-cc-pVTZ level of theory.

to be stretched to almost 1.2 Å, while *r*(AlH) shortens to within 0.1 Å of the equilibrium bond length. In this sense, the $Al^+/2H_2$ transition state lies closer to the covalent $AlH_2^+(H_2)$ than it does to $Al^+(H_2)_2$. In contrast, the corresponding transition state for $B^+/2H_2$ decreases about 45 kcal/mol (80% decrease) from the B^+/H_2 value and lies closer to $B^+(H_2)_2$, with *r*(BH) about 0.25 Å longer than the covalent equilibrium length and *r*(H_2) elongated to only about 0.87 Å.

The transition state for $Al^+/3H_2$ is essentially identical to that for $Al^+/2H_2$, with the third H_2 located more than 2.0 Å from Al^+. The binding energy of this H_2 to $Al^+/2H_2$ transition state is 3.9 kcal/mol, about midway between binding to the electrostatic complex (2.1 kcal/mol) and the inserted molecule (6.8 kcal/mol). Motion out of this transition state toward the covalent molecule proceeds through the same pericyclic mechanism operating in the $Al^+/2H_2$ system. The relatively large activation energy of 53.2 kcal/mol is certainly compatible with the experimental absence[6] of $AlH_2^+(H_2)_2$ in the thermal reaction of Al^+ with $3H_2$. This result differs markedly from $B^+/3H_2$, where $BH_2^+(H_2)_2$ formation was observed experimentally,[1] and the transition state involved all three H_2 molecules, equivalently dropping the activation energy to only 3.4 kcal/mol (70% decrease with respect to $B^+/2H_2$).

It is interesting to consider why the Al^+/nH_2 reactions parallel the B^+/nH_2 reactions for $n = 1$ and 2 but deviate strongly for $n = 3$. Figure 4 compares the HOMO of $Al^+/3H_2$ along the $B^+/3H_2$ reaction path up to the formation of the high-symmetry D_{3h} structure. The two electrostatic minima are very similar, both having C_3 symmetry and a HOMO that transforms as the totally symmetric, A representation. With a small distortion from this minima, the $B^+/3H_2$ arrives at the higher symmetry, C_{3v} transition state for which there is no corresponding $Al^+/3H_2$ stationary point. Here the HOMO of $B^+/3H_2$ still transforms as

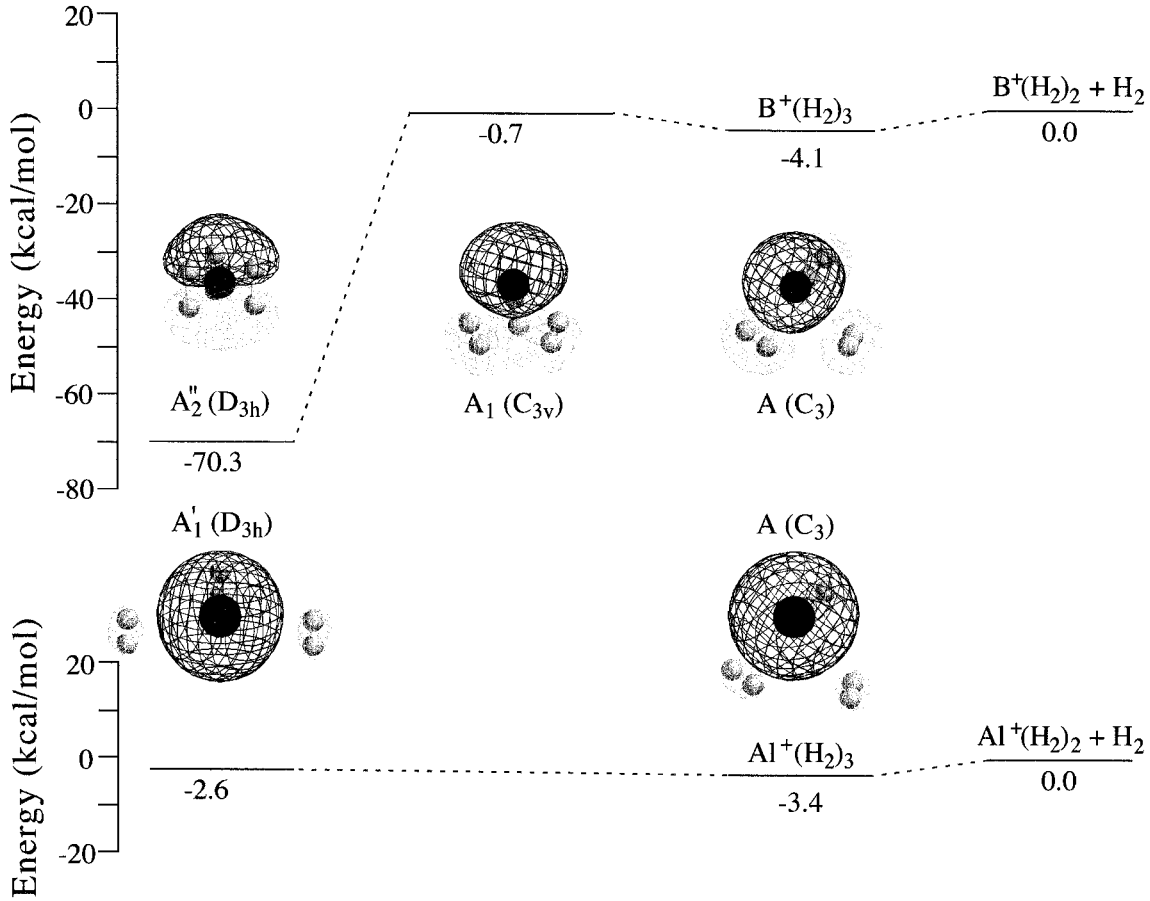

Figure 4. Comparison of the evolution of the highest occupied valence orbital for $Al^+(H_2)_2 + H_2 \rightarrow AlH_2^+(H_2)_2$ with $B^+(H_2)_2 + H_2 \rightarrow BH_2^+(H_2)_2$ along the minimum energy path from the electrostatic minimum to the lowest energy D_{3h} structure. Indicated energies are for the electronic surfaces without ZPE considerations. The energy scales do not apply to the orbitals.

a totally symmetric representation. However, at the D_{3h} stationary point, the HOMO of $B^+/3H_2$ transforms as the nontotally symmetric A_2'' representation, with the node that used to lie between B^+ and the three H_2 molecules now positioned on the horizontal reflection plane of the molecule, bisecting the three H_2 molecules. In contrast, the $Al^+/3H_2$ HOMO at the D_{3h} stationary point has A_1' symmetry with the molecular orbital node continuing to lie between the Al^+ and the three H_2 molecules. It is also clear that the low energy of the $B^+/3H_2$ D_{3h} structure arises from 3c−2e covalent bonding between B^+ and each H_2. This point is emphasized by H_2 bond length and stretching frequency that are more than 0.3 Å longer and 1900 cm^{-1} lower, respectively than their isolated molecular values. Alternatively, the D_{3h} structure for $Al^+/3H_2$ exhibits only electrostatic binding and at a level somewhat less than the C_3 electrostatic minimum.

Comparing the reaction energetics of Al^+/nH_2 to B^+/nH_2 suggests the substantial activation energy lowering observed with the addition of a second H_2 molecule, arising from the mechanistic change to a pericyclic reaction, may be a general result for a ns^2 electron configuration. However, the further substantial activation energy lowering with the addition of a third H_2 molecule, occurring for B^+ but not Al^+, suggests that this process requires the formation of 3c−2e bonds.

Acknowledgment. B.L. wishes to thank the Clark Scholars Program at Texas Tech University for a summer fellowship. We also gratefully acknowledge the support of the Robert A. Welch Foundation and the Petroleum Research Fund, administered by the American Chemical Society, under Grant No. 33631-AC6, for partial support of this work.

Supporting Information Available: Tables giving the geometries and harmonic frequencies of various $Al^+(H_2)_n$ and $AlH_2^+(H_2)_{n-1}$ stationary points (and their deuterated analogues) optimized at the MP2/aug-cc-pVTZ level of theory. This material is available free of charge via the Internet at http://pubs.acs.org.

References and Notes

(1) Kemper, P. R.; Bushnell, J. E.; Weis, P.; Bowers, M. T. *J. Am. Chem. Soc.* **1998**, *120*, 7577.
(2) Sharp, S. B.; Gellene, G. I. *J. Am. Chem. Soc.* **1998**, *120*, 7585.
(3) DePuy, C. H.; Gareyev, R.; Hankin, J.; Davico, G. E. *J. Am. Chem. Soc.* **1997**, *119*, 427.
(4) Rasul, G.; Olah, G. A. *Inorg. Chem.* **1997**, *36*, 1278.
(5) Cotton, F. A.; Wilkinson, G. *Advanced Inorganic Chemistry*, 5th ed.; Wiley-Interscience: 1987; Chapter 7.
(6) Kemper, P. R.; Bushnell, J.; Bowers, M. T.; Gellene, G. I. *J. Phys. Chem.* **1998**, *102*, 8590.
(7) Bu, Y.; Cao, Z.; Yang, Z. *Int. J. Quantum Chem.* **1995**, *55*, 329.
(8) Dunning, T. H., Jr. *J. Chem. Phys.* **1989**, *90*, 1007.
(9) Kendal, R. A.; Dunning, T. H., Jr.; Harrison, R. J. *J. Chem. Phys.* **1992**, *96*, 6796.
(10) Werner, H.-J.; Knowles, P. J. *J. Chem. Phys.* **1985**, *82*, 5053.
(11) Knowles, P. J.; Werner, H.-J. *Chem. Phys. Lett.* **1985**, *115*, 259.
(12) Werner, H.-J.; Reinsch, E. A. *J. Chem. Phys.* **1988**, *89*, 5803.
(13) Knowles, P. J.; Werner, H. *J. Chem. Phys.* Lett. **1988**, *145*, 514.
(14) Raghavachari, K.; Trucks, G. W.; Pople, J. A.; Head-Gordon, M. *Chem. Phys. Lett.* **1989**, *157*, 479.
(15) Langhoff, S. R.; Davidson, E. R. *Int. J. Quantum Chem.* **1974**, *8*, 61.
(16) Frisch, M. J.; Trucks, G. W.; Schlegel, H. B.; Gill, P. M. W.; Johnson, B. G.; Robb, M. A.; Cheeseman, J. R.; Keith, T.; Petersson, G. A.; Montgomery, J. A.; Raghavachari, K.; Al-Laham, M. A.; Zakrzewski, V. G.; Ortiz, J. V.; Foresman, J. B.; Peng, C. Y.; Ayala, P. Y.; Chen, W.; Wong, M. W.; Andres, J. L.; Replogle, E. S.; Gomperts, R.; Martin, R. L.;

Fox, D. J.; Binkley, J. S.; Defrees, D. J.; Baker, J.; Stewart, J. P.; Head-Gordon, M.; Gonzalez, C.; Pople, J. A. *Gaussian 94*, Revision B.3; Gaussian, Inc.: Pittsburgh, PA, 1995.

(17) MOLPRO is a package of ab initio programs written by H.-J. Werner and P. J. Knowles with contributions from J. Almlöf, R. D. Amos, M. J. O. Deegan, S. T. Elbert, C. Hampel, W. Meyer, K. Peterson, R. Pitzer, A. J. Stone, P. R. Taylor, and R. Lindh.

(18) Chang, D. T. Masters Thesis, Texas Tech University, 1998.

(19) Huber, K. P.; Herzberg, G. *Constants of Diatomic Molecules*; Van Nostrand Reinhold: New York, 1979.